[Frontiers In Bioscience, Scholar, 11, 105-121, March 1, 2019]

The collagen scaffold supports hiPSC-derived NSC growth and restricts hiPSC

Marzena Zychowicz[1], Krystyna Pietrucha[2], Martyna Podobinska[1], Malgorzata Kowalska-Wlodarczyk[3], Jacek Lenart[4], Justyna Augustyniak[1], Leonora Buzanska[1]

[1]Stem Cell Bioengineering Unit, Mossakowski Medical Research Centre Polish Academy of Sciences, Pawinskiego 5 St, 02-106, Warsaw, Poland, [2]Department of Material and Commodity Sciences and Textile Metrology, Lodz University of Technology, Zeromskiego 116 St, 90-924, Lodz, Poland, [3]Oil and Gas Institute, National Research Institute, 25 A Lubicz St, 31-503 Cracow, Poland, [4]Department of Neurochemistry, Mossakowski Medical Research Centre Polish Academy of Sciences, Pawinskiego 5 St, 02-106, Warsaw, Poland

TABLE OF CONTENT

1. Abstract
2. Introductions
3. Materials and Methods
- *3.1. Collagen dispersion and its temperature denaturation*
- *3.2. Synthesis of the scaffold and its characterization*
  - *3.2.1. Preparation of the scaffold*
  - *3.2.2. Differential scanning calorimetry (DSC)*
  - *3.2.3. Fourier transform infrared spectroscopy (FTIR-ATR) analysis*
  - *3.2.4. Porosity and distribution of pore size*
- *3.3. Human induced pluripotent stem cell culture and neural differentiation*
- *3.4. RNA isolation*
- *3.5. RT-PCR*
- *3.6. RNA integrity assay*
- *3.7. qRT-PCR*
- *3.8. Scaffold-cells co-culture*
- *3.9. Viability of cells cultured on collagen scaffolds*
- *3.10. Immunocytochemistry and confocal scanning laser microscopy*
- *3.11. Statistical analysis*

4. Results and Discussion
- *4.1. Properties of collagen derived from porcine tendons*
- *4.2. Insight in functional properties of 3D collagen scaffolds*
- *4.3. Characterization of lineage related hiPSC and hiPSC-derived neural stem cells in 2D cell culture*
- *4.4. hiPSC and hiPSC-NSC culture on collagen scaffolds*

5. Conclusions
6. Acknowledgments
7. References

1. ABSTRACT

The human induced pluripotent stem cells (hiPSC) are one of the promising candidates as patient specific cell source for autologous transplantation or modeling of diseases. The collagen (Col) scaffolds have been shown suitable to create *in vitro* biomimetic microenvironment for human neural stem cells, but their ability to accommodate stem cells at different stages of neural differentiation has not been verified yet. In this paper we compare lineage related hiPSC during neural differentiation for their ability to colonize Col scaffold. We have also focused on modification of collagen physicochemical properties with improved

mechanical and thermal stability, without loss of its biological activity. The hiPSC expressing markers of pluripotency (OCT4, SOX2, NANOG) after neural commitment are NESTIN, GFAP, PDGFR alpha, beta-TUBULIN III, MAP-2, DCX, GalC positive. We have shown, that Col scaffold was not preferable for hiPSC culture, while the neurally committed population after seeding on Col scaffolds revealed good adhesion, viability, proliferation, along with sustaining markers of neuronal and glial differentiation. The Col scaffold-based 3D culture of hiPSC-NSCs may serve as a research tool for further translational studies.

2. INTRODUCTION

The complex pathology of central nervous system (CNS), involving a cascade of secondary events and the formation of inhibitory barriers, hampers regeneration across the lesion site and often results in irreversible loss of motor function and has far reaching psychological and economic impacts to patients and healthcare systems (1). To date, there are no fully successful medical treatments with clinically documented efficacy to actively improve the repair of the human CNS. Nerve tissue engineering is a rapidly developing interdisciplinary field that involves the *in vitro* culturing of stem cells on biodegradable and biocompatible scaffold. Recently our lab and others have done significant works demonstrating the effectiveness of using collagen-based biomaterials to create the scaffolds for neurally committed stem cells (2–8).

In agreement with the experience of other authors e.g. (9,10) the role of collagen (Col), due to a very complex structure in the preparation of scaffolds for tissue engineering applications, has not been sufficiently clarified. It is known that Col can be extracted from a variety of animal sources. An accurate selection of Col source is important to prepare optimal combination of scaffold which could serve as a carrier for neural cells. The efficacy of Col scaffolds strongly depends on the kind/type of Col and, above all, on the reaction conditions and its modifications. It was recognized that Col extracted from mammalian sources, primarily bovine or porcine tendon or skin has the most similar properties with human Col (11). One major advantage of Col from pig sources in comparison to bovine is, that porcine Col has less susceptibility towards infection with transmitting pathogens (bovine spongiform encephalopathy, BSE, and transmissible spongiform encephalopathy, TSE) (12). The most commonly used extraction methods of Col are based on the solubility of raw material in neutral saline solutions, acid solutions or acid solutions with added enzymes (9). However, there has been little information available on the structural change of porcine Col during pepsin solubilisation (10-13). In our previous studies (3–5) Col was extracted from pig tendons by combined techniques, such as acid associated with digestion using pepsin. However, the some important physicochemical properties of such Col have not been tested. In particular, diagnostic efficacy of Col scaffolds as the *in vitro* biomimetic culture system is the most important area in which its reliability has not yet been adequately validated.

In light of these earlier researches, the aim of the present study was to characterize and identify the major constituents of Col isolated from fresh porcine tendon by pepsin digestion. Furthermore, an attempt was made to produce a stable three-dimensional (3D) Col scaffolds, using a simple chemical intervention (carbodiimide a “zero length” crosslinking agent) that would prepare the porous sponge with the best architecture (pore size, pore distribution) and biological properties. Functionalized 3D Col scaffolds have been further investigated as microenvironment mimicking natural extracellular matrix (ECM) for culturing human induced hiPSC and hiPSC-derived neurally committed progenitors. We hypothesized that Col scaffolds are very good carriers for hiPSC-derived neural stem cells (hiPSC-NSC) but not for non-differentiated, hiPSC. We have documented different, developmental stage dependent ability to adhere, survive and differentiate of hiPSC on the modified Col scaffolds: while acquiring neural phenotype hiPSC-derived neural cells start to adhere to the scaffolds and began to form neuronal networks.

3. MATERIALS AND METHODS

3.1. Collagen dispersion and its temperature denaturation

Col was derived from purified porcine Achilles tendons. The use of collagen isolated from porcine tendons was approved by the Local Commission of Ethics in Lodz, Poland (Resolution 4 / LB 505/2010).

Preparation of the Col dispersion was done in three steps presented here in brief:

- In the first step, mechanically disintegrated crude tendons were swollen in 10 % NaCl homogenized and filtered.
- In the second step, from the supernatant, Col was precipitated by adding 0.1. M Na_2HPO_4.
- In the third step, the precipitate was suspended in 0.1. M HCl with the addition of 0.4. % pepsin. Then, Col was precipitated by means of 0.0.2 M Na_2HPO_4, filtered off, washed with distilled water and finally dissolved in 0.5. M CH_3COOH.

The concentration of Col in dispersion was analysed by the determination of hydroxyproline (Hyp)

content according to the method recommended by the PN-ISO 3496:2000 Standard.

Temperature denaturation (T_d) of porcine Col in acetic acid solution was determined from temperature induced viscosity change, using an Ubbelohde viscometer type AVS 470 (Schott, Germany), according to the method described by Safandowska and Pietrucha (14). Briefly, the thermal denaturation curve was obtained by plotting the reduced viscosity against temperature. The T_d was expressed as a mid-point temperature between the extrapolated line for native Col (non-denatured) and that for fully denatured Col on the reduced viscosity *vs*. temperature plot. Each value was the mean of three determinations.

3.2. Synthesis of the scaffold and its characterization

3.2.1. Preparation of the scaffold

To remove entrapped air-bubbles, the Col dispersion at 0.7.3 % (w/v) was deaerated under reduced pressure and designed to create appropriate scaffold. Sponge-shape scaffold was obtained by freezing the dispersion of Col at -40 ºC. Then, the frozen dispersion was lyophilized at -55 ºC (Labconco, USA). To improve the functional properties of the scaffolds, Col sponges were modified according to previously described method (15,16) with significant modifications. Reaction crosslinking was carried out by immersing sponges in 70 % ethanol solution containing a mixture of 1-ethyl-3-(3-dimethyl aminopropyl) carbodiimide hydrochloride (EDC), morpholinomethane sulphonic acid (MES) and N-hydroxysuccinimide (NHS). After the crosslinking reaction, the sponges were immersed in Na_2HPO_4 and NaCl solutions, respectively. Subsequently, these products were thoroughly washed with deionized water. To prepare spongy 3D scaffolds, the matrices were refrigerated at -40 °C and subsequently lyophilized at -55 °C. Sponges without any crosslinking were used as controls.

3.2.2. Differential scanning calorimetry (DSC)

DSC measurements were carried out with a Q2000 device (TA Instruments, USA) calibrated with indium. The samples of Col scaffolds weighed of about 10 mg were heated from 20°C to 300 °C at a rate of 10ºC min^{-1} in nitrogen atmosphere. T_d was determined at the mid-point of the transition peak, and the temperature at the start of the process was measured at the onset peak. The experiment was performed three times in triplicate.

3.2.3. Fourier transform infrared spectroscopy (FTIR-ATR) analysis

The FTIR investigation was performed using a Nicolet 6700 spectrometer, utilizing the attenuated total reflectance (ATR) technique. The absorption spectral range was collected between 4000 cm^{-1} and 600 cm^{-1}, with a spectral resolution of 4 cm^{-1}. At least three spectra for scaffolds with and without control were carried out and analyzed.

3.2.4. Porosity and distribution of pore size

The porosity, pore size distribution were determined by mercury porosimetry using an AutoPore IV 9500 V1.0.9 (Micromeritics) equipped with a suitable computer system. Technical solutions were based on the cylindrical model of pore space, in which the pore space is simulated as a group of cylindrical capillaries that transport reservoir fluids. The distribution of the equivalent pore diameters and their distribution in the examined pore space was obtained from Washburn's equation (17):

$$d = -4\tau \times \cos(phi)/ P \quad (1)$$

where: d is the pore diameter, P is the applied pressure, phi is the contact angle between the rock and the reservoir fluid, and τ is the surface tension. The proportional distribution of pores of a given diameter in the pore space was determined by counting the partial volumes of mercury injected into a sample. Because the mass of the sample, its external volume, and the volume of the rock skeleton were known while measuring the porosity, it was computed the results obtained with Washburn's equation and obtained the distribution of pore diameters in the given sample and partial volumes as well as the dynamic porosity of the sample, its skeleton density and bulk density. The cumulative curve was obtained for the following relationship: applied pressure – volume of mercury.

3.3. Human induced pluripotent stem cell culture and neural differentiation

The hiPSC line, derived from CD34+ cord blood cells by episomal, non-integrating with genome system, was purchased from Thermo Fisher Scientific (Gibco® Human Episomal iPSC Line, Life Technologies), and maintained in feeder free and serum free conditions. Human iPS cells were cultured on vitronectin (Thermo Fisher Scientific) in Essential 8 (E8) medium (Thermo Fisher Scientific) and were passaged at 70 percent confluency with daily medium change. The neural commitment of hiPSC was performed according to (18) with some modifications (19) until the stage of neural stem cells. Briefly, hiPSC were detached as aggregates using EDTA, collected and transferred to 6 well vitronectin-coated plates in E8 medium in cell concentration of $3x10^5$ cell/well. One day after of iPSC splitting the E8 medium was changed to neural induction medium comprised of Neural Induction Supplement (1:50) and Neurobasal (both from Thermo Fisher Scientific) and this medium was changed every other day until the 100% confluency

was reached. On day 7th of neural induction cells were harvested and replated on Matrigel-coated plates as single cell suspension of $1x10^5$ cells/cm^2 in neural expansion medium (Neural Induction Supplement and 1:1 Neurobasal and Advanced DMEM (Thermo Fisher Scientific) and cells were maintained in this medium as human induced pluripotent stem cell- derived neural stem cells (hiPSC-NSC) and used for further experiment after passage 6.

3.4. RNA isolation

hiPSC and hiPSC-NSC seeded as 2D culture on vitronectin or Matrigel (respectively)-coated 6 well plates were prepared for RNA isolation after they reach 70% confluency. ZR-DuetTM DNA/RNA Mini Prep Kit (Zymo Research) was used for total RNA extraction from hiPSC and hiPSC-NSC according to the manufacturers' protocols, after this step RNA was purified by treatment with DNAse (Clean-Up RNA Concentrator kit; A&A Biotechnology, Gdynia, Poland) for elimination of genomic DNA from samples. The concentration of RNA was evaluated by measuring the absorbance at 260 nm using a NanoDrop ND-1000 spectrophotometer (Thermo Fisher scientific, Waltham, USA). Total RNA purity was determined by calculating the A_{260}/A_{280} absorbance ratio.

3.5. RT-PCR

2 µg of RNA was used to synthesize first-strand cDNA with High-Capacity RNA-to-cDNA™ Kit, (Thermo Fisher Scientific). RT-PCR reaction was performed with Taq DNA Polymerase (EURx, #EK2500-02P) according to the manufacturer's instructions. Primers used in this study are shown in Table 2. Each time *ACTB* was used as a control of proper course and confirmation of the presence of template cDNA in the reaction mixture. RT-PCR has been performed with cDNA obtained from 2D cell culture of hiPSC and hiPSC-NSC. All experiments were performed at least three times, "+/-" means that not all repetitions (but at least two) were positive for the expression of tested gene.

3.6. RNA integrity assay

To evaluate messenger RNA (mRNA) integrity status and to eliminate degraded RNA from qRT-PCR analysis, the 3′/5′ integrity assay was performed. This 3′/5′ approach is based on the measurement of the relative expression of two amplicons located on the 3′ and 5′ regions of a house-keeping gene. Two assays were designed along the length of the TBP (TATA-box binding protein) cDNA. One is located close to the 3' UTR and the second is approximately 1 kb upstream close to 5' end. RNA integrity index was assessed by calculation (Cq) of difference between qRT-PCR products amplified with the 5' and 3' primers pars. The method of cDNA synthesis has been described previously. Sequences of TBP3' and TBP5' primers are presented in Table 4. All primers were designed in the Primer-BLAST; (https://www.ncbi.nlm.nih.gov/tools/primer-blast/ and quantified *in silico* in the Sequence Manipulation Suite (http://www.bioinformatics.org/sms2/index.html); UNAFOLD tool (http://eu.idtdna.com/UNAFold) and uMELT (Melting Curve Predictions Software; https://www.dna.utah.edu/umelt/umelt.htm). Primers have been synthesized in the Laboratory of DNA Sequencing and Oligonucleotide Synthesis, Institute of Biochemistry and Biophysics Polish Academy of Sciences, (http://oligo.pl/).

3.7. qRT-PCR

The real time reaction was performed with 5µL (10ng) of cDNA template in 25 µL of reaction mixture containing 12.5. µL of iTaq™ universal SYBR® Green Supermix (Bio-rad) and 0.25 µmol/L each primer on the LightCycler® 96 (Roche Diagnostics GmbH, Mannheim, Germany). The amplification program included an initial denaturation step at 95°C for 3min, 40 cycles of denaturation at 95°C for 10 sec, and annealing/extension at 60°C for 1 min. All samples were tested in triplicate. The quantification cycle (Cq) values automatically calculated by the LightCycler® 96 software was then used for data analysis (GeneEx 6.1. software (MultiD Analyses AB, Göteborg, Sweden). The candidates for reference gene validation were described in our previous papers (19, 20). The primers used in qRT-PCR are presented in Table 4. The qRT-PCR gene analysis was performed on the material collected from 2D cell culture of hiPSC and hiPSC-NSC for the genes: *POU5F1, SOX2, NANOG, NES, MAP2, NEFL, GFAP, and CSPG4* (Chondroitin Sulfate Proteoglycan 4, marker of early oligodendrocytes). For the reference genes validation studies, primers for following genes were used: *ACTB* - Actin Beta; *GAPDH* - Glyceraldehyde-3-Phosphate Dehydrogenase; *HPRT1* - Hypoxanthine Phosphoribosyltransferase 1; *TUBB3* - beta Tubulin class III (BTUB); *EID2* - EP300 Interacting Inhibitor Of Differentiation 2; *CAPN10* - Calpain 10, Calcium-Activated Neutral Proteinase 10; *RABEP2* - Rabaptin, RAB GTPase Binding Effector Protein 2; *ZNF324B* - Zinc Finger Protein 324B; *NAT1* -N-Acetyltransferase1; *TBP* - TATA-Box Binding Protein; *PHB* –Prohibitin; *UBC* - Ubiquitin C; *CCNG1* - Cyclin G1; *MYC* - Myc Avian Myelocytomatosis Viral Oncogene Homolog; *EEF1A1* - Eukaryotic Translation Elongation Factor 1 Alpha 1.

3.8. Scaffold-cells co-culture

Samples of sterilized Col scaffolds were cut on 2x2x2 mm pieces and placed in Eppendorf tubes, where hiPSC or hiPSC-NSC were added as cell suspension ($2,5x10^6$ cells/ml) and left in incubator overnight. Next day samples of cells-seeded scaffolds

were placed in the 24-well plate in 0,5ml of fresh medium: Essential 8 for hiPSC and neural expansion medium for hiPSC-NSC.

3.9. Viability of cells cultured on collagen scaffolds

After 1, 3 or 5 days of culture scaffolds seeded with either hiPSC cells or hiPSC-derived neural stem cells were gently washed with pre-warmed PBS and placed in solution of 2 μM calcein and 4 μM ethidium homodimer 1 for 30 minutes (Live/Dead® Viability/ Cytotoxicity Kit, Thermo Fisher Scientific). After this time samples were immediately visualized in confocal microscope (Confocal Laser Microscope LSM 510, Zeiss).

3.10. Immunocytochemistry and confocal scanning laser microscopy

After 6 days of culture samples were gently washed with PBS, fixed with 4%PFA for 20 minutes, permeabilised with 0,1% Triton X-100 for 15 minutes (this step was omitted for the cell surface antibodies). Following blocking with 10% goat serum for 1h, the primary antibodies were used overnight: TRA1-60 (mouse IgM, 1:100 Millipore), SSEA3/4 (mouse IgG3, 1:100, Millipore), OCT4 (mouse IgG2b, 1:200, Santa Cruz) – for hiPSC; and beta-TUBULIN III (mouse IgG2a, 1:1000, Sigma Aldrich), NESTIN (mouse IgG1, 1:300, Millipore), NF200 (mouse IgG1, 1:400, Sigma Aldrich), MAP2 (mouse IgG1, 1:500, Sigma Aldrich), DOUBLECORTIN (DCX, rabbit polyclonal, 1:500, Cell Signalling Technology), A2B5 (mouse IgM, 1:300, Millipore), GalC (mouse IgG3, 1:200, Millipore), NG2 (mouse IgG1, 1:100, Santa Cruz), GFAP (rabbit polyclonal, 1:500, Dako) and Ki67 (mouse IgG1, 1:500, Leica/Novocastra) for hiPSC-NSC cultured on Matrigel-covered coverslip in 24-well plate and hiPSC-NSC cultured on scaffolds. After 3x washing with PBS relevant secondary antibodies (goat anti mouse Alexa 488 or 546, goat anti rabbit H+L Alexa 488 or 546) were used for 1h in RT. Following gently washing with PBS cell nuclei were stained with Hoechst 33258 and samples were gently washed with PBS and immersed in Fluorescence Mounting Medium (Dako). The visualisation was made in the Laboratory of Advanced Microscopy Techniques, Mossakowski Medical Research Centre Polish Academy of Sciences using Confocal Laser Microscope LSM 510 (Zeiss) and Zen Blue software.

3.11. Statistical analysis

The data from qRT-PCR obtained from hiPSC and hiPSC-NSC were analyzed in the GeneEx 6.1. software (Multid Analyses AB, Göteborg, Sweden). The results from 3 independent experiments, each in 4 replicates. The data from qRT-PCR analysis were presented in the bar graph. The results on the bar graph are presented as Fold Change (FC, fold change value was calculated from ΔΔCq method for a gene expressed in hiPSC-NSC vs. hiPSC). Relative quantification in real-time RT-PCR was performed according to Pfafl methods (21). NormFinder, was used for reference gene prediction. RNA samples were classified as degraded when RNA integrity index, calculated as ΔCq TBP products amplified with the 5' and 3' primers pars, was smaller than ΔCq <1.0. Results presented on the graph (Figure 7) are given as the mean with standard error of measurement (SEM). Data in the text are shown as the mean with standard deviation (SD).

4. RESULTS AND DISCUSSION

Structural protein-Col has unique properties for the bio-medical applications including neural tissue engineering. The main problem with such structural protein is that its extraction from natural sources destroys, to some extent, macro-scale structure. Thus, new methods are needed to subsequently rebuild structural protein into the required shapes and sizes without losing their unique properties. It is very important that the reconstituted Col has bio-mechanical and biological properties similar to that of the native Col, while containing no toxic or bio-incompatible agents. In this study, as a result of limited proteolysis of Col materials with pepsin and purification by differential salt precipitation, among others, non-collagenous elements could be removed. Telopeptide parts of the terminal of the Col macromolecule having antigenic properties are also removed by these treatments.

4.1. Properties of collagen derived from porcine tendons

Among other, thermal stability is an important property of Col when used in biomaterial applications. The effect of digesting Col with pepsin on its thermal stability as a curve illustrating the course of protein denaturation is shown in Figure 1.

On the basis of measurements, it can be seen (Figure 1) that porcine Col exhibits two T_d of 34.8. and 39.5. ºC, respectively. It seems that under given conditions there is a certain number of Col destruction fragments or unfolding of Col helical structure resulting in loss of viscosity and lowering of T_d. However, a higher T_d value indicates that the Col under study retains an integral super helix structure, and the pepsin solubilisation method used allows the reconstitution of the native Col structure. These results are in accordance with those of porcine skin Col solubilised by pepsin (22) but are slightly lower than the T_d of bovine Col (23). It is understandable that bovine collagen, as compared to porcine Col, generally contains more Hyp, which significantly influences the T_d increase.

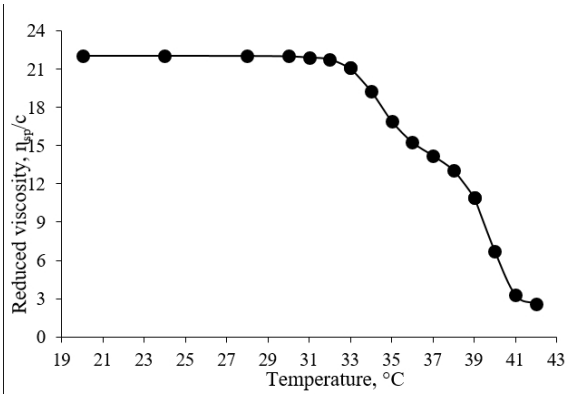

Figure 1. Thermal denaturation curve of porcine collagen. The denaturation temperature was measured by viscosity change in 0.1.5 M acetic acid of collagen solution. The incubation time at each temperature was 30 min at the given temperature from 20 to 50ºC, and then the efflux time (t) was recorded. The efflux times (to) of 0.15 M acetic acid solution (collagen solvent) was also determined under the same conditions. The reduced viscosity (????sp/c), where ????sp is the specific viscosity and is calculated by (t-to)/to and c is the concentration of the samples, was plotted against the temperature.

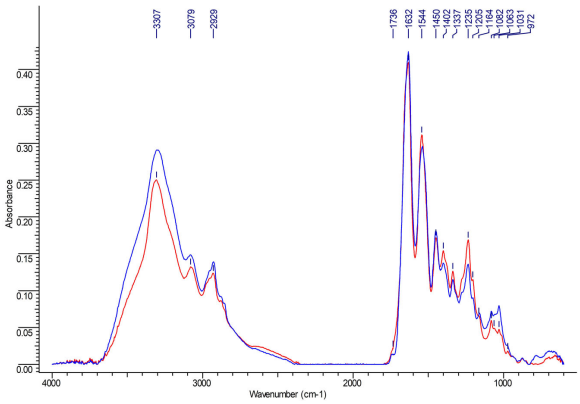

Figure 2. FTIR-ATR spectra of collagen unmodified and modified sponges. Blue line denotes non-crosslinked collagen; red line denotes collagen crosslinked by EDC/NHS.

4.2. Insight in functional properties of 3D collagen scaffolds

To fabricate porous 3D Col scaffolds, of various methods such as freeze-drying (24,25), electrospinning (26,27) and embossing ice particulates (28) were applied. Resent, more comprehensive data on modification of Col for biomedical applications are published in excellent review article (29). In our lab, we developed a freeze-drying process and a technique involving use of EDC with NHS to catalyse the formation of “zero-length” covalent crosslinks between Col macromolecules. We (16,30) and others (15) previously discussed the crosslinking reaction of Col in detail, which may be ascribed to the possible occurrence of fundamental reaction. EDC/NHS conjugates carboxylates Glu and Asp acid residues of Col to ε-amine groups from the Lys or Hyl residues of Col to form peptide bonds without the addition of toxic catalysts. However, the physicochemical and biological properties of such Col scaffolds were not sufficiently investigated.

Col scaffolds can possess poor biological activity or be highly bioactive, depending on the conformation of Col triple helices, among others. The changes in the helical structure of Col macromolecules due to the modification by EDC/NHS were evaluated using FTIR spectroscopy (Figure 2). The FTIR spectrum of non-crosslinked Col did not significantly differ from that of crosslinked Col (Fig.2.); these infrared spectra are almost super-imposable and exhibit several characteristic absorption bands that fit the range for other Cols (16,31). Importantly, the FTIR absorption ratios between 1234 cm^{-1} (amide III) and 1450 cm^{-1} (pyrolidonic ring) of both Col unmodified and Col modified were approximately equal to 0.9.8 and 0.8.1, respectively (Table 1).

This phenomenon (Table 1) clearly indicate that EDC/NHS react with Col but the secondary structure of the Col triple helix is preserved. This finding suggests that an intact triple helix conformation ensures good Col scaffold bioactivity. The typical A_{1239}/A_{1452} absorbance ratios for denatured Col are close to 0.6. (32).

The life processes and responses to the microenvironmental cues as well as differentiation potential of stem cells seeded inside the Col scaffold are controlled not only by the composition of the scaffold material, but also by the inner 3D architecture of the sponges. The functional properties of biomedical materials designed for nerve tissue repair are strongly depend both on the simple porosity, i.e. the ratio between the empty volume and the total volume, and by the pore size and pore distribution. In this study the porosity of Col sponges without or with cross-linking by EDC/NHS exhibited the high porosity of 96.5. and 94 %, respectively. However, it has been proven by other group (33) that, four types of Col scaffold prepared with ice particulates had similar porosity and interconnectivity, but differently sized pores. Therefore, it is very important to study here the size and distribution of pores, primarily. The results presented in Figure 3 show the pore size distribution of Col network characterized using mercury porosimetry method.

As can be seen (Figure 3), the curves for unmodified and modified Col are not super-imposable. Analysis of the quantitative measurements revealed that the largest fraction, which comprises at least 75 % of the total pore volume of the crosslinked sponge, is occupied by pores ranging from 10-120 μm in size. This pores size range appears to be adequate for neural cells attachment and growth (34). The results

Table 1. Effect of collagen crosslinking on FTIR absorption ratio between 1235 cm^{-1} and 1450 cm^{-1}

Parameter	Sponge unmodified		Sponge modified by EDC/NSH	
Wavenumber, cm-1	1235	1450	1235	1450
Absorbance	0.1689	0.1718	0.1380	0.1701
Ratio A_{1235}/A_{1450}	0.98		0.81	

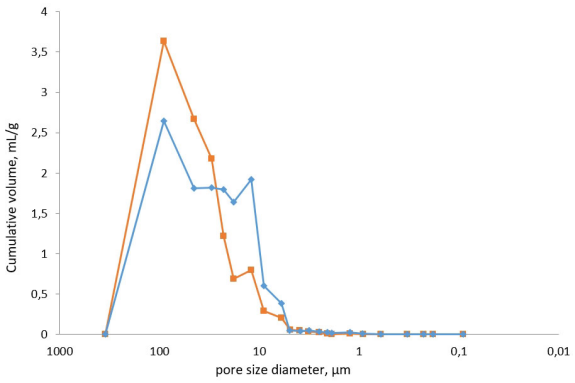

Figure 3. Pore size distribution of the collagen-based network of unmodified and modified sponges using EDC/NHS method crosslinking. Red line denotes unmodified sponges; blue line denotes modified sponges.

obtained in this study agree with those as visualized by scanning electron microscope (SEM), which revealed that regenerative scaffolds based on Col have a narrowly specified pore structure with a pore diameter range of 20-125 µm (16,35,36). Nevertheless, for unmodified sponge, approximately 80 % of total pore volume of the sponge, is occupied by pore ranging 40-200 µm. Generally, comparing Col sponges crosslinked with EDC/NHS to Col unmodified sponges clearly demonstrated that the pore structure (pore size, pore distribution) of Col crosslinked sponges was significantly lower. This finding suggests that crosslinking offers more intermolecular bonds that form more junction points, which in turn affects the microarchitecture of pores. Moreover, the Col scaffolds crosslinked via EDC/NHS process after freeze-drying due to the introducing covalent crosslinks between the polypeptide chains of the Col fibers had significantly increased resistance to temperature (Figure 4).

4.3. Characterization of lineage related hiPSC and hiPSC-derived neural stem cells in 2D cell culture

In standard two dimensional culture of hiPSC in serum free and feeder free conditions (Figure 5A) cells express pluripotency markers, such as OCT4, TRA1-60 and SSEA3/4, shown by immunocytochemistry (Figure 5B-D). The same cell population was also checked for the expression of genes involved in pluripotency and differentiation at mRNA level (Table 3). Data from RT-PCR have revealed, that hiPSC express genes related and involved in maintaining of the pluripotency state, like: *POU5F1* (*OCT4), SOX2, REX1, NANOG* but also (however at low level) genes involved in ectodermal (*SOX17*), endodermal (*AFP, FOX2A*) and mesodermal (*TBXT,BRACHYURY)* differentiation. This indicate, that some cells are undergoing spontaneous differentiation into tissues from three germ layers.

Inducing of neural differentiation, caused gradual loss of expression of pluripotency genes (*POU5F1, REX1, NANOG*) as well as endodermal (*AFP, FOX2A*) and mesodermal (*BRACHYURY*) markers, while increased expression of ectodermal (*SOX17, PAX6*) genes was observed.

The stimulation of neural commitment in the culture of iPSC by applying Neural Induction Medium (NIM) changes rapidly the shape of the colonies and the morphology of the cells within colonies. The typical compact colonies of pluripotent cells (Figure 6 A) are no longer regular and more loose inside with small cells separated (Figure 6 B-C), Further incubation of cells for 6 days in NIM results with dense, 100% confluent culture (Figure 6D).

Immunocytochemical analysis of cells replared on Matrigel after at least 6 following passages revealed the presence of cells with neural morphology, which are branched, with extended protrusions, expressing abundantly at the protein level NESTIN – the indicator of neural commitment as well as neuronal markers such as: beta-TUBULIN III, NF200, DOUBLECORTIN (DCX) and in some of the cells MAP2 (Figure 6E). We have also observed small population of cells, which express markers of glial differentiation, like PDGFR alpha and GalC but were negative for NG2. The presence of Ki67-positive cells, indicates that the hiPSC-NSC is a mixed population of cells more advanced in differentiation and progenitors still able to proliferate (Figure 6E). The effectiveness of differentiation process was confirmed by RT-PCR analysis. In the neurally committed cells - hiPSC-NSC, expression of *TUBB3, MAP2, NES, NEUROG2, PDGFRA* as well as *NEFL, NEUROG1, ND1* and a weak expression of astrocytic *GFAP* gene was observed (Table 3).

The expression of selected genes shown by RT-PCR (Table 3) was further evaluated by qRT-PCR

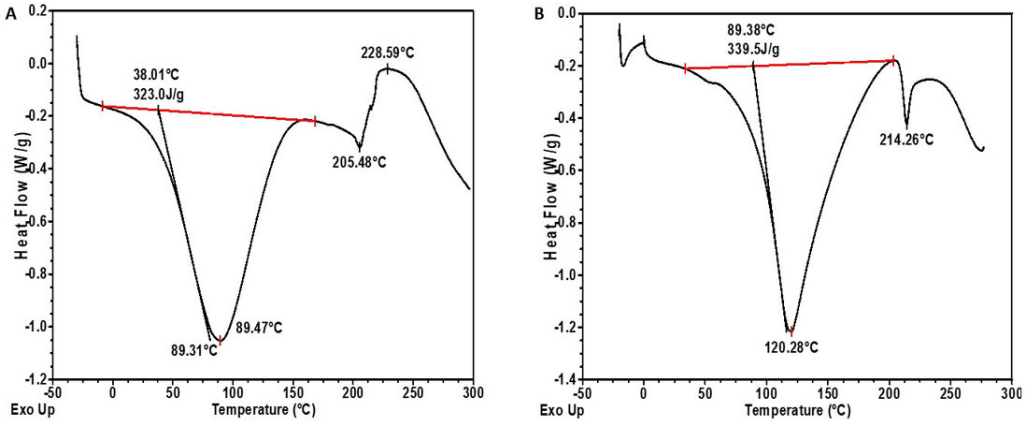

Figure 4. DSC thermograms of collagen 3D scaffolds: (A) collagen sponge un-crosslinked, (B) collagen sponge crosslinked by EDC/NHS.

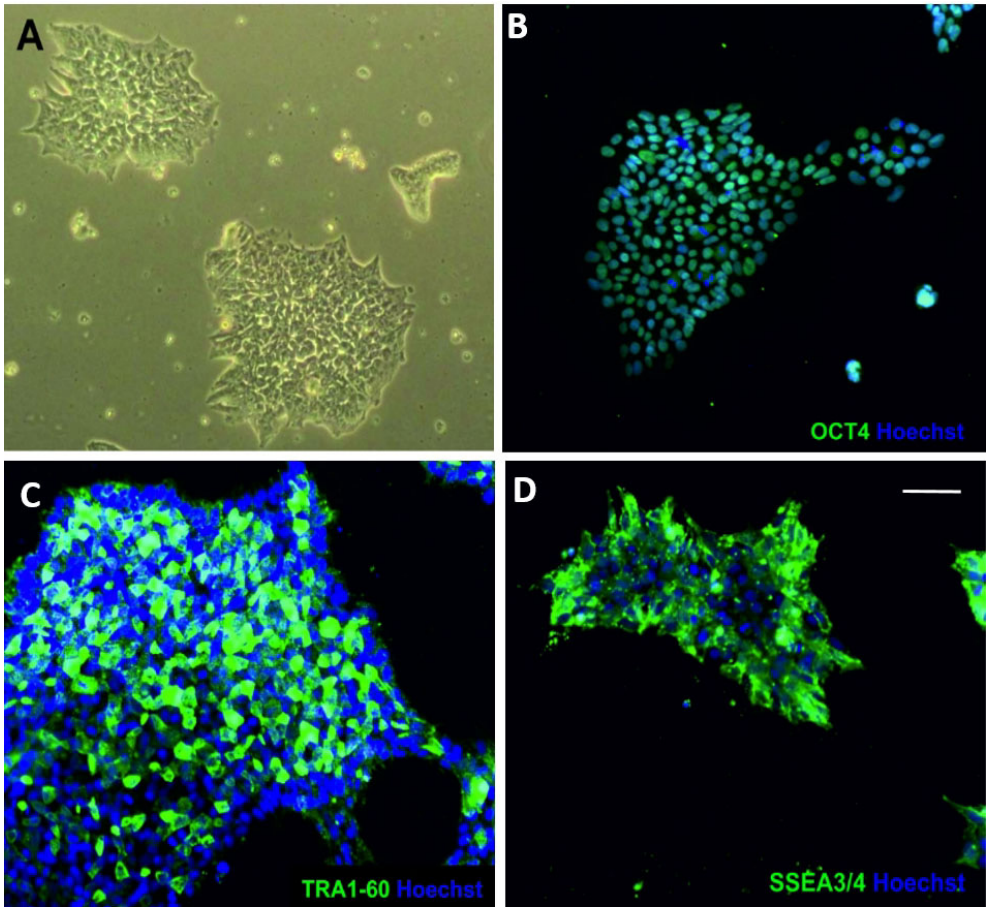

Figure 5. Phase contrast image of standard hiPSC cultured on vitronectin (A) and immunocytochemical analysis for the presence of main pluripotency markers: nuclear marker OCT4 (B) and cell surface markers TRA1-60 (C) and glycosphingolipid stage-specific embryonic antigen 3/4 (SSEA3/4, D). Scale bar is 50 micrometers.

(Figure 7), which allowed for the comparison of the dynamic changes in the expression of genes during differentiation. To ensure high quality of the results obtained from qRT-PCR we have used the integrity assay to eliminate degraded mRNA from further qRT-PCR analysis.

HiPSC-NSC was characterized by loss of expression of the main pluripotency markers: *POU5F1* - gene encoding *OCT4* protein (-12.26±0.20) and *NANOG* (-5.89±0.59), while relatively low expression of third key factor in the regulation of pluripotency and neural differentiation - *SOX2* (0.25±0.39), as

Table 2. Primers used for RT-PCR

Primers	Genbank number	Primer sequence	Amplicon length (bp)
POU5F1 F	NM_002701.5.	CTCCTGGAGGGCCAGGAATC	381
POU5F1 R		CCACATCGGCCTGTGTATAT	
SOX 2 F	NM_003106.3.	ACACCAATCCCATCCACACT	224
SOX 2 R		GCAAACTTCCTGCAAAGCTC	
REX1 F	XM_011531607.2.	GCTGCCCTGAGAAAGCATCT	289
REX1 R		GCGTTAGGATGTGGGCTTTC	
NANOG F	XM_011520850.1.	TCCAGGATTTTAACGTTCTGCT	580
NANOG R		TTCTTGCATCTGCTGGAGGC	
AFP F	NM_001354717.1.	GAATGCTGCAAACTGACCACGCTGGAAC	281
AFP R		TGGCATTCAAGAGGGTTTTCAGTCTGGA	
FOX2A F	NM_021784.4.	TCATGCCAGCGCCCACGTACGACGAC	216
FOX2A R		TGGGAGCGGTGAAGATGGAAGGGCAC	
SOX17 F	NM_022454.3.	CGCTTTCATGGTGTGGGCTAAGGACG	186
SOX17 R		TAGTTGGGGTGGTCCTGCATGTGCTG	
PAX6 F	NM_001310161.1.	ACCCATTATCCAGATGTGTTTGCCCGAG	317
PAX6 R		ATGGTGAAGCTGGGCATAGGCGGCAG	
TBXT F	XM_011536080.2.	GCCCTCTCCCTCCCCTCCACGCACAG	274
TBXT R		CGGCGCCGTTGCTCACAGACCACAGG	
MSX1 F	NM_002448.3.	CGAGAGGACCCCGTGGATGCAGAG	307
MSX1 R		GGCGGCCATCTTCAGCTTCTCCAG	
TUBB3(beta-TUBULIN III)F	NM_001197181.1.	CTCAGGGGCCTTGGACATC	159
TUBB3(beta-TUBULIN III)R		CAGGCAGTCGCAGTTTTCAC	
NEFL F	XM_011530200.2.	GAGGAACACCAAGTGGGAGA	160
NEFL R		TTCTGGAAGCGAGAAAGGAA	
MAP 2 F	XM_017004140.1.	CAGGTGGCGGACGTGTGAAAATTGAGAGTG	212
MAP 2 R		CACGCTGGATCTGCCTGGGGACTGTG	
NES F	NM_006617.1.	TGGCTCAGAGGAAGAGTCTGA	169
NES R		TCCCCCATTTACATGCTGTGA	
NEUROG1 F	NM_006161.2.	CTTGAGACCTGCATCTCCGAC	679
NEUROG1 R		GCGTTGTGTGGAGCAAGTCTT	
NEUROG2 F	NM_024019.3.	CGCATCAAGAAGACCCGTAG	173
NEUROG2 R		GTGAGTGCCCAGATGTAGTTGTG	
ND1 F	NM_002500.4.	CGCTGGAGCCCTTCTTTG	118
ND1 R		GCGGACGGTTCGTGTTTG	
GFAP F	NM_002055.4.	GGCCCGCCACTTGCAGGAGTACCAGG	328
GFAP R		CTTCTGCTCGGGCCCCTCATGAGACG	
PDGFRA F	NM_001347830.1.	ATCAATCAGCCCAGATGGAC	891
PDGFRA R		TTCACGGGCAGAAAGGTACT	
(ACTB) F	NM_001101.4	GCCAACCGCGAGAAGATGA	120
(ACTB) R		CATCACGATGCCAGTGGTA	

F- forward; R-reverse

Table 3. RT-PCR analysis of expression of pluripotency and differentiation genes in hiPSC, and hiPS-derived NSC

Gene name	hiPSC	hiPSC- derived NSC
POU5F1 (OCT4)	+	-
SOX2	+	+
REX1	+	-
NANOG	+	-
AFP	+/-	-
FOXA2	+/-	-
SOX17	+	+
PAX6	-	+
TBXT (T BRACHURY)	+/-	-
MSX1	-	-
TUBB3(beta-TUBULIN III)	-	+
NEFL (NF200)	-	+
MAP2	-	+
NES(NESTIN)	-	+
NEUROG1	-	+
NEUROG2	-	+
ND1	-	+
GFAP	-	+/-
PDGFRA(PDGFRalpha)	+	+
ACTB(beta-ACTIN)	+	+

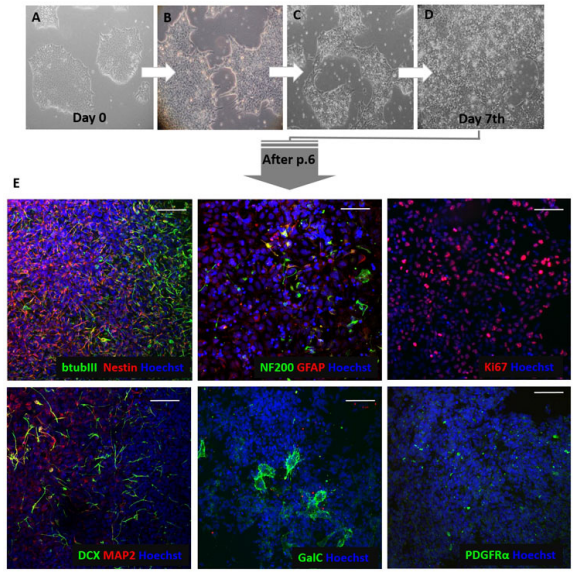

Figure 6. Contrast phase images of neural induction of hiPSC (A-D) and immunocytochemical analysis of hiPSC-NSC (E). On day 0 hiPSC are seeded on vitronectin in Essential 8 medium (A), one day after, when the cells are at 15-25% confluency culture medium is changed for medium dedicated for neural induction (B), during following days fresh neural induction medium is added to the culture, colonies are inspected under the microscope for proper neural morphology (C) and at day 7 culture become 100% confluent (D) obtaining population of neural stem cells at passage 0. Then, cells are passaged and maintained in neural expansion medium for cryopreservation or expansion. After six passages hiPSC-NSCs exhibit markers of neuronal and glial differentiation (E) and are subjected for experiments. Scale bar is 50 micrometers.

compared to hiPSC. The *POU5F1* and *NANOG* gene expression was strongly down regulated in the hiPSC-NSC population (Figure 7). The loss of expression of *POU5F1* upon neural differentiation of hiPSC was also observed in our previous study in the more advanced stage of neural differentiation: early neural progenitors (eNP) and neural progenitors (NP) (20), what indicates that this population has no potential for teratoma formation and might be safe for possible future therapeutic applications, however this would need further evaluation in functional tests.

Expression of *NES* (NESTIN) - early neural marker, was up-regulated in hiPSC-NSC population (3.18±0.71). Among the neural genes, the strongest expression was observed for *MAP2* (4.04±0.62) and *NEFL* gene (4.09±0.20). We have checked also glial differentiation by verification of presence of early oligodendrocyte progenitor marker *CSPG4* and key astrocyte marker *GFAP* (Figure 7). We have observed slight (not statistically significant) down-regulation of expression of *CSPG4* (-1.72±0.32) in hiPSC-NSC, as compared to hiPSC and this marker was not detected at the protein level by the immunocytochemical analysis. On the other hand, the expression of GalC, another oligodendroglial marker, was present in the population of hiPSC-NSC (Figure 6E.) suggesting that population of human neural stem cells obtained in this study can be further differentiated into all three neural cell types: neurons, astrocytes and oligodendrocytes. The expression of *GFAP* (-1.72±0.33) in the culture of hiPSC-NSC was weakly up-regulated (data not statistically significant). However, we have detected GFAP-positive cells by immunocytochemistry (Figure 6E), what indicates that applied protocol promote neuronal differentiation, notwithstanding enable to obtain some small amount of astro- or oligodendroglial cells. We have also searched for the best reference gene to perform qRT-PCR in tested populations (normalization of results in hiPSC-NSC *vs* hiPSC). As shown on Figure 8, the best reference gene (as was suggested to use by *NormFinder* for normalization calculations) was found to be *RABEP2*.

4.4. hiPSC and hiPSC-NSC culture on collagen scaffolds

The cells at the pluripotent stage – hiPSC, cultured in 2D on vitronectin-coated or Matrigel-coated culture flasks grow in the form of compact colonies (Figure 6A). However, when these cells are seeded onto Col scaffold they do not adhere to the surface of scaffold and at 1st day after seeding they aggregate forming cell clumps (Figure 9A). After 5 days of culture on the scaffold, staining for pluripotent markers TRA-1-60 revealed only few positive cells and the same was found for the marker of proliferation (Ki67, Figure 9B, C). Live-dead staining of hiPSC performed on the scaffold, revealed that at day 1 of cell culture some living cells adhered to the collagen but during the

Table 4. Primers used for qRT-PCR

Primers	*Genbank number*	*Primers sequence*	*Amplicon length (bp)*
POU5F1 F	NM_002701.5	GAGAGGGGTTGAGTAGTCCCTT	100
POU5F1 R		CGAAATCCGAAGCCAGGTGTC	
SOX2 F	NM_003106.3	CGGAAAACCAAGACGCTCAT	140
SOX2 R		TAACTGTCCATGCGCTGGTT	
NANOG F	NM_024865.3	AATAACCTTGGCTGCCGTCT	150
NANOG R		AGCCTCCCAATCCCAAACAAT	
NES F	NM_006617.1	CCCCGTCGGTCTCTTTTCTC	96
NES R		TCGTCTGACCCACTGAGGAT	
MAP2 F	NM_002374.3	TGCCTCAGAACAGACTGTCAC	101
MAP2 R		AAGGCTCAGCTGTAGAGGGA	
NEFL F	NM_006158.4	AGCGTGGGAAGCATAACCAG	80
NEFL R		CTGGTCTGTAAACCGCCGTA	
GRFAP F	NM_002055.4	GTGAAGACCGTGGAGATGCG	76
GFAP R		TGCCTCACATCACATCCTTGT	
CSPG4 F	NM_001897.4	GCAAATCCCAGGTGCTGTTC	105
CSPG4 R		CGTCCAGGAGGGTGAACATT	
ACTB F	NM_001101.3	GCTCACCATGGATGATGATATCGC	169
ACTB R		CACATAGGAATCCTTCTGACCCAT	
GAPDH F	NM_002046.5	GTTCGACAGTCAGCCGCATC	90
GAPDH R		TCCGTTGACTCCGACCTTCA	
HPRT1 F	NM_000194.2	AGGCGAACCTCTCGGCTTTC	166
HPRT1 R		CTGGTTCATCATCACTAATCACGAC	
TUBB3 F	NM_006086.3	CAACCAGATCGGGGCCAAGTT	146
TUBB3 R		GAGGCACGTACTTGTGAGAAGA	
EID2 F	NM_153232.3	GGCATCGCTCTGTCCAGTTA	74
EID2 R		GCTTGGACATCTCAGACCGT	
CAPN10 F	NM_023083.3	TCTCACCGGGCTACTACCTG	86
CAPN10 R		CCCGGTAGAGAAGACTCGGA	
RABEP2 F	NM_024816.2	AGGAAGGGGCAAATGGTGAG	96
RABEP2 R		CAGCCTTCATGGTTTCCATTTCTG	
ZNF324B F	NM_207395.2	CATTGGAAGGACAAACCTAGGATGATG	164
ZNF324B R		CTTATCTGCTCCAAAGCTATCACTGTC	
NAT1 F	NM_001160170.3	TGGTTGCCGGCTGAAATAAC	93
NAT1 R		TCTGTCTAGGCCAGTCTCCT	
TBP F	NM_003194.4	GCAAGGGTTTCTGGTTTGCC	80
TBP R		CAAGCCCTGAGCGTAAGGTG	
PHB F	NM_001281496.1	TGGAAGCAGGTGAGAATGGAG	76
PHB R		ATCATGGAGCAGAGGAGGACT	
UBC F	NM_021009.6	ACGGGACTTGGGTGACTCTA	82
UBC R		ATCGCCGAGAAGGGACTACT	
CCNG1 F	NM_004060.3	GCCTCTCGGATCTGATATCGT	138
CCNG1 R		CATTCAGCTGGTGTAGCAGT	

MYC F	NM_002467.4	CCCTCCACTCGGAAGGACTA	96
MYC R		GCTGGTGCATTTTCGGTTGT	
EEF1A1 F	NM_001402.5	TGTTCCTTTGGTCAACACCGA	122
EEF1A1 R		ACAACCCTATTCTCCACCCA	
TBP_F5	NM_003194.4	GCCCGAAACGCCGAATATAA	141
TBP_R5		TGCCAGTCTGGACTGTTCTT	
TBP_F3	NM_003194.4	CCGGCTGTTTAACTTCGCTT	66
TBP_R3		GAAACAGTGATGCTGGGTCA	
RPLP0 F	NM_001002.3	CCTCGTGGAAGTGACATCGT	76
RPLP0 R		CTGTCTTCCCTGGGCATCAC	

F- forward; R-reverse

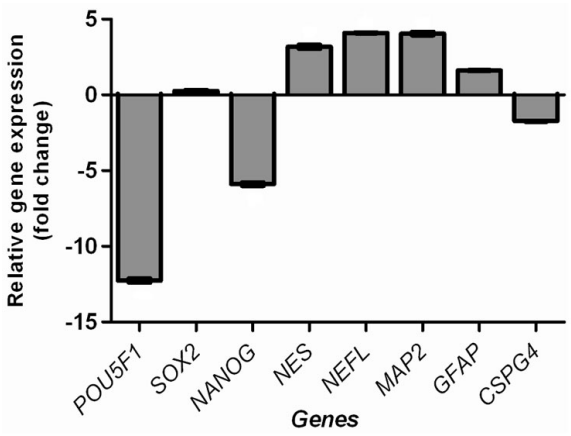

Figure 7. Real time (qRT-PCR) expression of genes involved in neural differentiation in hiPSC-NSC. Gene expression is shown as a fold changes of NSC vs hiPSC (C). A relative expression of pluripotency markers (*POU5F1, SOX2, NANOG*); early neural marker (*NES*); neuronal markers (*MAP2, NEFL*); astrocytic marker (*GFAP*) and oligodendrocytic marker, (*CSPG4*) were represented as the mean (SEM) from three independent experiments, each in 4 replicates. test The data from qRT-PCR analysis were presented in the bar graph. The results on the bar graph have been shown as FC (fold change value have been calculated from ΔΔCq method for a gene expressed in hiPSC-NSC vs. hiPSC).

subsequent days of culture most of these cells do not survive (Figure 10 upper panel). However, the culture of neurally committed cells (hiPSC-NSC) on the collagen scaffold (Figure 10 lower panel) revealed, that the cells survive and, even after 5 days in culture on the scaffold, high viability with small amount of dead cells is observed.

The population of hiPS-NSC seeded and cultured on collagen scaffolds express early neural: beta-TUBULIN III, NESTIN and glial A2B5 markers. The cells preferentially grow in clusters, which resemble the structure of neurospheres, observed in NSC culture from different sources (37), with a core of undifferentiated cells inside, and cells expressing neural markers outside (Figure 11). Moreover, throughout the time of culture, neuronal and glial markers are expressed, what indicates that three dimensional culture did not inhibit cell's ability to differentiate (Figure 11A-F). Some of the cells expressing beta-TUBULIN III extend very long protrusions, while other, less differentiated express also Ki67 and are still able to proliferate (Figure 11A). In the tested population of cells growing in three dimensional culture on Col scaffold only weak staining of astrocytic marker GFAP (Figure 11B) is observed. However in the same population some of the cells express more immature glial protein A2B5 (Figure 11D), as well as NESTIN (Figure 11C), indicating neural stemness of these cells.

On the 3D view of the confocal Z-stack (Figure 11E and F) we can observe, that cells were present both on surface, as well as inside scaffold structure, what proofs the ability of the neurally committed cells to migrate through the scaffold. Neurally committed stem cells have been shown before to penetrate and accommodate Col-DAC and Col-CS scaffolds (4). Interestingly, astrocytic marker – GFAP, present in 2D culture of hiPSC-NSC is only sporadically observed on the Col scaffolds tested in this study. Similar results were obtained by our group for the collagen scaffolds functionalized with chondroitin sulfate Cs (Col-CS), while the 3D collagen scaffold modified by crosslinking agent 2,3-dialdehyde cellulose (Col-DAC) was permissive for the maintenance of cells expressing astrocytic markers (4). On the other hand, neuronal beta-TUBULIN III expressing cells are present abundantly and colonize the scaffold at its all layers, expanding long protrusions, what is typical for establishing of the functional, neuronal network. This effect is similar to described previously by our group, where neuronal network was obtained on keratin associated proteins-based 3D scaffold (37). Thus, our present data and obtained before (4) suggest preferential support of different Col scaffolds for neuronal lineage differentiation, than maintaining cells in pluripotent stage. Primarily it was found, that hiPSC could survive and retain expression of pluripotency marker in thermoreversible 8–10% (wt/vol) poly(N-isopropylacrylamide)-co-poly(ethylene

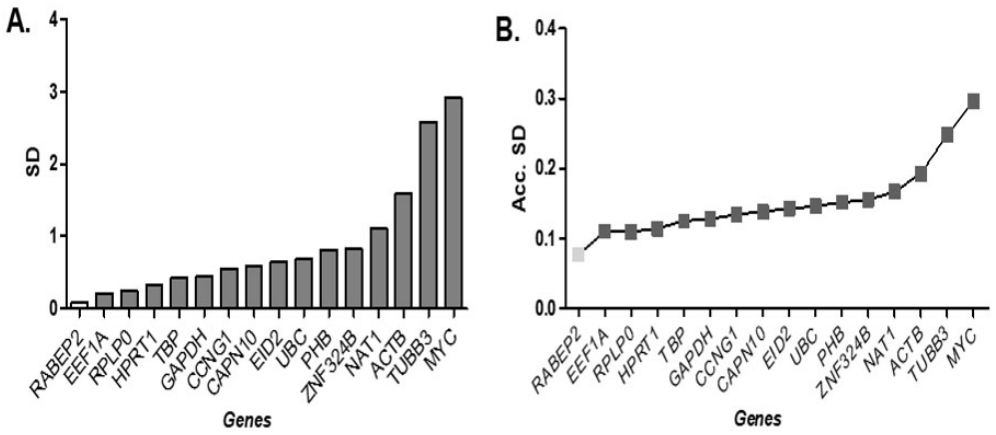

Figure 8. Validation of housekeeping genes in hiPSC and hiPSC-NSC using NormFinder algorithm. A) The stability of gene expression: the lowest values correspond to the most stable genes. B) Determination of the optimal number of reference genes for normalization for NSC and hiPSC is based on the calculation of the Average accuracies (Acc.) and their standard deviations (SD) (Acc. S.D). As a result of normalization procedure the NormFinder algorithm suggested to use one reference gene RABEP2.

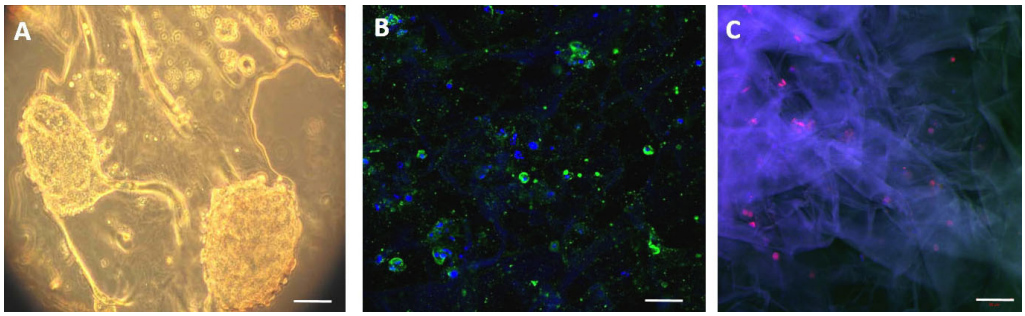

Figure 9. Human iPS cells seeded onto collagen scaffolds. Contrast phase micrograph of hiPS after one day in culture (A). Immunocytochemical staining of hiPS cells for TRA-1-60 (green, B) and Ki67 (red, C) after 5 days of culture on collagen scaffold. blue-cell nuclei stained with Hoechst. Scale bar is 50 micrometers.

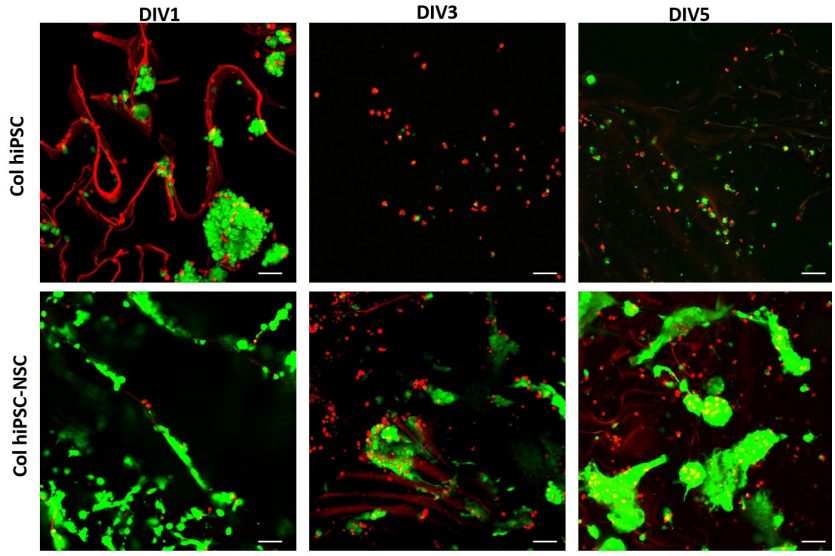

Figure 10. Live-dead staining of hiPSC and hiPS-NSC cells cultured on Col scaffold. Living cells are stained for calcein (green) while dead cells are stained for ethidium homodimer-1 (red). Imaging after 1 and 5 days of *in vitro* (DIV) culture. Scale bar is 50 micrometers.

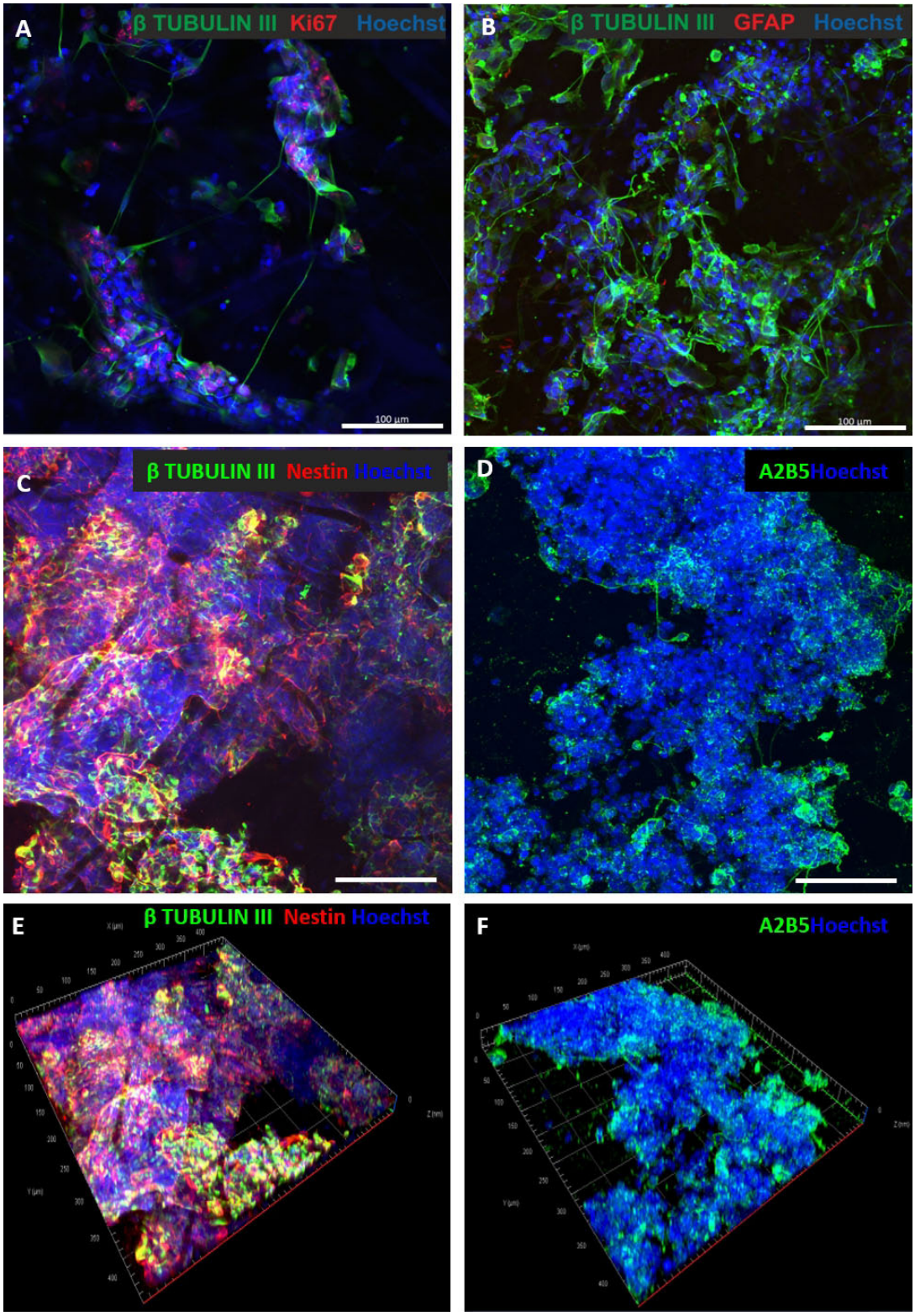

Figure 11. Immunocytochemical analysis of hiPSC derived NSC cultured for 6 days on the scaffold for expression of: beta-TUBULIN III, Ki67, GFAP, A2B5 and NESTIN. Cells are contra stained with Hoechst to visualize cell nuclei. Note that beta-TUBULIN III expressing cells can extend very long protrusions forming neuronal network (A,B), while other, less differentiated express also Ki67 and are still able to proliferate (A). GFAP is expressed only sporadically (B), while NESTIN (C) and A2B5 (D) is present abundantly in ihPSC-NSC caltured on Col scaffold. The images of Col scaffold seeded with hiPSC-NSC and stained for beta-TUBULIN III/NESTIN and A2B5 (C and D, respectively), captured by confocal laser scanning microscope (Z-stack), were powered by Arivis, ZEN2.3. lite blue edition creating three dimensional views of the image (E and F), indicating the presence and the migration of cells through the scaffolds. Scale bar is 100 micrometers.

glycol) (PNIPAAm-PEG) hydrogel (38). However, collagen based scaffolds have also been implicated in long-term, feeder-free culture of the cells in pluripotent stage. The latter was shown in culture platform involving co-immobilization of heparin–catechol (HepC) and collagen type-1 (Col) (39) and the authors indicated heparin's affinity toward a wide range of proteins as the main support for undifferentiated *in vitro* growth of hESC. Recently attention of some research groups is focused on the tunable cell-derived extracellular matrix (40) and its mechanotransduction properties in the maintenance of the human cells at their pluripotent stage.

5. CONCLUSIONS

The functional properties of 3D Col scaffolds were modulated by adjusting the crosslink density of the sponges during fabrication. Importantly, crosslinking using EDC/NHS offers more intermolecular bonds that form more junction points, which in turn affects the microarchitecture of pores and increases thermal stability without changing the secondary structure of the Col triple helix conformation. Such properties of these scaffolds are required to cells attachment and proliferation.

For the cell-biomaterial co-culture we have used neural stem cells derived from human induced pluripotent stem cell line (hiPSC-NSC), and these cells express neuronal as well as glial markers, what was confirmed by qRT-PCR and immunostaining. While the obtained in this study Col scaffold was an efficient carrier for neurally committed cells enabling their proliferation as well as their further differentiation, it was not suitable for the adhesion and maintenance of pluripotent, non-differentiated hiPSC long term culture.

6. ACKNOWLEDGMENTS

Marzena Zychowicz and Krystyna Pietrucha equally contribute to this paper. The authors declare that they have no conflict of interest. The work was supported by Wroclaw Research Centre EIT+ under the project „Biotechnologies and advanced medical technologies" – BioMed (POIG.01.0.1.0.2-02-003/08) financed from the European Regional Development Fund (Operational Programme Innovative Economy, 1.1.2.)"; and statutory funds to MMRC. The authors would like to thank Dr. M. Chrzanowski and Dr. S. Sztajnowski for providing the DSC and FTIR facilities.

7. REFERENCES

1. NR Iyer, TS Wilems, SE Sakiyama-Elbert: Stem cells for spinal cord injury: Strategies to inform differentiation and transplantation. *Biotechnol Bioeng* 114, 245–259 (2017) DOI: 10.1002/bit.26074

2. AR Murphy, A Laslett, CM O'Brien, NR Cameron: Scaffolds for 3D in vitro culture of neural lineage cells. *Acta Biomater* 54, 1–20 (2017) DOI: 10.1016/j.actbio.2017.02.046

3. J Drobnik, K Pietrucha, M Kudzin, K Mader, J Szymański, A Szczepanowska: Comparison of various types of collagenous scaffolds applied for embryonic nerve cell culture. *Biologicals* (2017) DOI; 10.1016/j.biologicals.2017.01.001

4. K Pietrucha, M Zychowicz, M Podobinska, L Buzanska: Functional properties of different collagen scaffolds to create a biomimetic niche for neurally committed human induced pluripotent stem cells (iPSC). *Folia Neuropathol* 2, 110–123 (2017) DOI: 10.5114/fn.2017.68578

5. J Drobnik, K Pietrucha, L Piera, J Szymański, A Szczepanowska: Collagenous scaffolds supplemented with hyaluronic acid and chondroitin sulfate used for wound fibroblast and embryonic nerve cell culture. *Adv Clin Exp Med* 26, 223-230 (2017)

6. X Li, S Liu, Y Zhao, J Li, W Ding, S Han, B Chen, Z Xiao, J Dai: Training Neural Stem Cells on Functional Collagen Scaffolds for Severe Spinal Cord Injury Repair. *Adv Funct Mater* 30, 265-271 (2016) DOI: 10.1002/adfm.201601521

7. H Duan, X Li, C Wang, P Hao, W Song, M Li, W Zhao, Y Gao, Z Yang: Functional hyaluronate collagen scaffolds induce NSCs differentiation into functional neurons in repairing the traumatic brain injury. *Acta Biomater* 45, 182-195 (2016) DOI: 10.1016/j.actbio.2016.08.043

8. KF Huang, WC Hsu, JK Hsiao, GS Chen, JY Wang: Collagen-Glycosaminoglycan Matrix Implantation Promotes Angiogenesis following Surgical Brain Trauma. *Biomed Res Int* 2014, 672409 (2014) DOI: 10.1155/2014/672409

9. MM Schmidt, RCP Dornelles, RO Mello, EH Kubota, MA Mazutti, AP Kempka, IM Demiate: Collagen extraction process. *International Food Research Journal* 23, 913-922 (2016)

10. H Yang, Z Shu: The extraction of collagen protein from pigskin. *J Chem Pharm Res* 6, 683-687 (2014)

11. MB Fauzi, Y Lokanathan, BS Aminuddin, BHI Ruszymah, SR Chowdhury: Ovine tendon collagen: Extraction, characterisation and fabrication of thin films for tissue engineering applications. *Mater Sci Eng C* 1, 63-171(2016)
DOI: 10.1016/j.msec.2016.05.109

12. R Parenteau-Bareil, R Gauvin, S Cliche, C Gariépy, L Germain, F Berthod: Comparative study of bovine, porcine and avian collagens for the production of a tissue engineered dermis. *Acta Biomater* 7, 3757-65 (2011)
DOI; 10.1016/j.actbio.2011.06.020

13. YK Lin, TY Lin, HP Su: Extraction and characterisation of telopeptide-poor collagen from porcine lung. *Food Chem* 1241, 583-1588 (2011)
DOI: 10.1016/j.foodchem.2010.08.018

14. M Safandowska, K Pietrucha: Effect of fish collagen modification on its thermal and rheological properties. *Int J Biol Macromol* 53, 32-7 (2013)
DOI: 10.1016/j.ijbiomac.2012.10.026

15. LHH Olde Damink, PJ Dijkstra, MJA Van Luyn, PB Van Wachem, P Nieuwenhuis, J Feijen: Cross-linking of dermal sheep collagen using a water-soluble carbodiimide. *Biomaterials* 17, 765-73 (1996)
DOI: 10.1016/0142-9612(96)81413-X

16. K Pietrucha: Physicochemical properties of 3D collagen-CS scaffolds for potential use in neural tissue engineering. *Int J Biol Macromol* 80, 732–739 (2015)
DOI: 10.1016/j.ijbiomac.2015.07.005

17. EW Washburn: Note on a Method of Determining the Distribution of Pore Sizes in a Porous Material. *Proc Natl Acad Sci* 7, 115-6 (1921)
DOI: 10.1073/pnas.7.4.115

18. Y Yan, S Shin, BS Jha, Q Liu, J Sheng, F Li, M Zhan, J Davis, K Bharti, X Zeng, M Rao, N Malik, MC Vemuri: Efficient and rapid derivation of primitive neural stem cells and generation of brain subtype neurons from human pluripotent stem cells. *Stem Cells Transl Med* 2, 862–70 (2013)
DOI: 10.5966/sctm.2013-0080

19. J Augustyniak, J Lenart, M Zychowicz, G Lipka, P Gaj, M Kolanowska, PP Stepien, L Buzanska: Sensitivity of hiPSC-derived neural stem cells (NSC) to Pyrroloquinoline quinone depends on their developmental stage. *Toxicol Vitr* 45, 434–444 (2017)
DOI: 10.1016/j.tiv.2017.05.017

20. J Augustyniak, J Lenart, M Zychowicz, PP Stepien, L Buzanska: Mitochondrial biogenesis and neural differentiation of human iPSC is modulated by idebenone in a developmental stage-dependent manner. *Biogerontology* 18, 665–677 (2017)
DOI: 10.1007/s10522-017-9718-4

21. MW Pfaffl: A new mathematical model for relative quantification in real-time RT-PCR. *Nucleic Acids Res* 29, 45e–45 (2001)
DOI: 10.1093/nar/29.9.e45

22. X Liu, N Dan, W Dan: Preparation and characterization of an advanced collagen aggregate from porcine acellular dermal matrix. *Int J Biol Macromol* 88,179-88 (2016)
DOI: 10.1016/j.ijbiomac.2016.03.066

23. K Pietrucha, S Verne: Synthesis and characterization of a new generation of hydrogels for biomedical applications. In: World Congress on Medical Physics and Biomedical Engineeringr, Eds: O Dössel, WC Schlegel, Munich (2009)

24. H Schoof, J Apel, I Heschel, G Rau: Control of pore structure and size in freeze-dried collagen sponges. *J Biomed Mater Res* 58, 352-7 (2001)
DOI: 10.1016/j.ijbiomac.2016.03.066

25. GS Offeddu, JC Ashworth, RE Cameron, ML Oyen: Structural determinants of hydration, mechanics and fluid flow in freeze-dried collagen scaffolds. *Acta Biomater* 1, 193-203 (2016)
DOI: 10.1016/j.actbio.2016.05.024

26. J Cheng, Y Jun, J Qin, SH Lee: Electrospinning versus microfluidic spinning of functional fibers for biomedical applications. *Biomaterials* 114, 121-143 (2017)
DOI: 10.1016/j.biomaterials.2016.10.040

27. KH Shin, JW Kim, YH Koh, HE Kim: Novel self-assembly-induced 3D plotting for macro/nano-porous collagen scaffolds comprised of nanofibrous collagen filaments. *Mater Lett* 143, 265-268 (2015)
DOI: 10.1016/j.matlet.2014.12.119

28. YG Ko, N Kawazoe, T Tateishi, G Chen: Preparation of novel collagen sponges using an ice particulate template. *J Bioact Compat*

Polym 25, 360-373 (2010)
DOI: 10.1177/0883911510370002

29. X Yu, C Tang, S Xiong, Q Yuan, Z Gu, Z Li, Y Hu: Modification of Collagen for Biomedical Applications: A Review of Physical and Chemical Methods. *Curr Org Chem* 20, 1797-1812 (2016)
DOI: 10.2174/1385272820666151102213025

30. E Marzec, K Pietrucha: The effect of different methods of cross-linking of collagen on its dielectric properties. *Biophys Chem* 132, 89-96 (2008)
DOI: 10.1016/j.bpc.2007.10.012

31. K Pietrucha, M Safandowska: Dialdehyde cellulose-crosslinked collagen and its physicochemical properties. *Process Biochem* 50, 2105-2111 (2015)
DOI: 10.1016/j.procbio.2015.09.025

32. AMDG Plepis, G Goissis, DK Das-Gupta: Dielectric and pyroelectric characterization of anionic and native collagen. *Polym Eng* 22, 203-91998 (1998)

33. Q Zhang, H Lu, N Kawazoe, G Chen: Pore size effect of collagen scaffolds on cartilage regeneration. *Acta Biomater* 10, 2005-13 (2014)
DOI: 10.1016/j.actbio.2013.12.042

34. AP Balgude, X Yu, A Szymanski, R V Bellamkonda: Agarose gel stiffness determines rate of DRG neurite extension in 3D cultures. *Biomaterials* 22, 1077-84 (2001)
DOI: 10.1016/S0142-9612(00)00350-1

35. IV Yannas: Emerging rules for inducing organ regeneration. *Biomaterials* 34, 321-30 (2013)
DOI: 10.1016/j.biomaterials.2012.10.006

36. K Pietrucha, E Marzec, M Kudzin: Pore structure and dielectric behaviour of the 3D collagen-DAC scaffolds designed for nerve tissue repair. *Int J Biol Macromol* 92, 1298-1306 (2016)
DOI: 10.1016/j.ijbiomac.2016.08.029

37. M Jurga, AW Lipkowski, B Lukomska, L Buzanska, K Kurzepa, T Sobanski, A Habich, S Coecke, B Gajkowska, K Domanska-Janik Generation of functional neural artificial tissue from human umbilical cord-blood stem cells. Tissue Eng Part C Methods. 2009 Sep;15(3):365-72
DOI: 10.1016/j.tiv.2005.06.036

38. Y Lei, DV Schaffer: A fully defined and scalable 3D culture system for human pluripotent stem cell expansion and differentiation. *Proc Natl Acad Sci U S A* 24, E5039-48 (2013)
DOI: 10.1073/pnas.1309408110

39. M Lee, Y Kim, JH Ryu, K Kim, YM Han, H Lee: Long-term, feeder-free maintenance of human embryonic stem cells by mussel-inspired adhesive heparin and collagen type I. *Acta Biomater* 1, 138-148(2016)
DOI: 10.1016/j.actbio.2016.01.008

40. IG Kim, CH Gil, J Seo, SJ Park, R Subbiah, TH Jung, JS Kim, YH Jeong, HM Chung, JH Lee, MR Lee, SH Moon, K Park: Mechanotransduction of human pluripotent stem cells cultivated on tunable cell-derived extracellular matrix. *Biomaterials* 150, 100-111 (2018)
DOI: 10.1016/j.biomaterials.2017.10.016

Abbreviations: *POU5F1(OCT4* – transcription factor, *POU* Class 5 Homeobox 1; *REX1* – RNA Exonuclease 1 Homolog; *NANOG* - transcription factor, Homeobox protein NANOG; *SOX2* – transcription factor, SRY -Box 2; early endodermal markers: *AFP* – homo sapiens alpha fetoprotein; *SOX17* –SRY (Sex Determining Region Y) box 17; *FOXA2* - Homo sapiens forkhead box A2; early mesodermal markers: *TBXT* – T Brachyury Transcription Factor; *MSX1* - Msh homeobox 1; early neuroectodermal marker*: PAX6* - Paired box protein, transcription factor present during embryonic development; *NES* – Nestin, early neural marker; neuronal markers: *MAP2* - Microtubule-Associated Protein 2; *NEFL* – Neurofilament Light Polypeptide; *ND1* - Neuronal Differentiation 1; *NEUROG2* - Neurogenin 2; *TUBB3* - beta Tubulin class III (BTUB*);* glial markers*: GFAP*- Glial Fibrillary Acidic Protein, marker of astrocytes–; *PDGFRA* - platelet-derived growth factor receptor A, marker of early oligodendrocytes; reference gene - *ACTB* - Actin Beta).

Key Words: hiPSC, Neural stem cells, Collagen, Scaffolds, Biomaterial

Send correspondence to: Leonora Buzanska, Stem Cell Bioengineering Unit, Mossakowski Medical Research Centre, Polish Academy of Sciences, Pawinskiego 5 str, 02-106 Warsaw, Poland, Tel: 48226086449, Fax: 48226685532, E-mail: buzanska@imdik.pan.pl